



Development and application of a population physiologically based pharmacokinetic model for penicillin G in swine and cattle for food safety assessment

Miao Li, Ronette Gehring, Jim E. Riviere, Zhoumeng Lin*

Institute of Computational Comparative Medicine (ICCM), Department of Anatomy and Physiology, College of Veterinary Medicine, Kansas State University, Manhattan, KS 66506, USA



ARTICLE INFO

Article history:

Received 8 March 2017

Received in revised form

6 June 2017

Accepted 13 June 2017

Available online 13 June 2017

Keywords:

Physiologically based pharmacokinetic (PBPK) model

Food safety

Food animal residue avoidance databank (FARAD)

Penicillin

Drug residue

Extralabel withdrawal interval

ABSTRACT

Penicillin G is a widely used antimicrobial in food-producing animals, and one of the most predominant drug residues in animal-derived food products. Due to reduced sensitivity of bacteria to penicillin, extralabel use of penicillin G is common, which may lead to violative residues in edible tissues and cause adverse reactions in consumers. This study aimed to develop a physiologically based pharmacokinetic (PBPK) model to predict drug residues in edible tissues and estimate extended withdrawal intervals for penicillin G in swine and cattle. A flow-limited PBPK model was developed with data from Food Animal Residue Avoidance Databank using Berkeley Madonna. The model predicted observed drug concentrations in edible tissues, including liver, muscle, and kidney for penicillin G both in swine and cattle well, including data not used in model calibration. For extralabel use (5× and 10× label dose) of penicillin G, Monte Carlo sampling technique was applied to predict times needed for tissue concentrations to fall below established tolerances for the 99th percentile of the population. This model provides a useful tool to predict tissue residues of penicillin G in swine and cattle to aid food safety assessment, and also provide a framework for extrapolation to other food animal species.

© 2017 Elsevier Ltd. All rights reserved.

1. Introduction

Penicillin G is an antimicrobial widely used to treat infectious diseases caused by penicillin-sensitive bacteria, including bacterial pneumonia and upper respiratory infection in food-producing animals, such as swine, cattle, sheep and horses (FDA, 2013b; Portis et al., 2012; Vogel et al., 2001). In the United States, it is approved to be used in swine and cattle (FDA, 2013b). Different formulations of penicillin G are approved for cattle and swine, including procaine salts for intramuscular (IM) administration in both swine and cattle, and benzathine salts for IM and subcutaneous (SC)

Abbreviations: AUC, area under the time concentration curve; FARAD, Food Animal Residue Avoidance Databank; IM, intramuscular; LOD, limit of detection; NSC, normalized sensitivity coefficient; PBPK, physiologically based pharmacokinetic; SC, subcutaneous; WDI, withdrawal interval; WHO, World Health Organization.

* Corresponding author. 1800 Denison Avenue, P200 Mosier Hall, Manhattan, KS 66506, USA.

E-mail addresses: miaoli@ksu.edu (M. Li), rgehring@ksu.edu (R. Gehring), jriviere@ksu.edu (J.E. Riviere), zhoumeng@ksu.edu (Z. Lin).

<http://dx.doi.org/10.1016/j.fct.2017.06.023>

0278-6915/© 2017 Elsevier Ltd. All rights reserved.

administrations in swine and cattle (Ranheim et al., 2002).

Animal-derived products with drug residues above the regulatory safe level (termed violative residues) challenge the global food safety (Baynes and Riviere, 2014; Baynes et al., 2016). The regulatory safe level, which is the maximum acceptable level of veterinary drugs in food products, is defined as the tolerance in the US and as the maximum residue level (MRL) in other countries. Penicillin G is one of the most predominant drug residues in animal-derived food products. In 2014, the USDA National Residue Program reported violative levels of penicillin G in 306 samples, which accounted for 22% of the total number of violations (USDA, 2015). To ensure animal-derived food safety, the US FDA has established a 0.05 µg/g tolerance for the penicillin G residues in edible tissues of cattle, and zero tolerance, which is operationally equivalent to the limit of detection (LOD), in edible tissues of swine and milk products (FDA, 2013b). In the United States, IM administration of procaine penicillin G is approved at a daily dose of 6600 IU/kg of body weight (6.5 mg/kg) for no more than 7 consecutive days, and in Canada it is 7500 IU/kg (7.4 mg/kg) (Papich et al., 1993).

Due to the development of reduced sensitivity to penicillin in bacteria since its initial approval several decades ago and the fact

that beta-lactamase can be saturated and overcome by administering higher doses, penicillin has become one of the drugs most commonly used at extralabel doses to remain effective (Chiesa et al., 2006). The extralabel (also called off-label) use of veterinary drugs is the way to use a drug in an animal under the supervision of veterinarians in the manner that is not accordance with the approved labeling of the drug, including the differences in dosage levels, frequencies, routes of administration, and others (FDA, 2017). Compared to the approved dose, much higher doses have been administered in practice. Doses of procaine penicillin G needed to effectively treat bovine respiratory disease have been reported as being 45,000 IU/kg (44.6 mg/kg) daily (Bateman et al., 1990). Typically used clinical doses for intramuscular treatment are approximately 3.5 and 10 times the US label dose (Payne et al., 2006). The extralabel use of penicillin G can lead to residues that are higher than concentrations considered safe for human consumption if the animals are slaughtered at the label withdrawal period. Therefore, it is necessary to develop a robust model to predict tissue residues and estimate extended withdrawal intervals (WDI) for the extralabel use of penicillin G in swine and cattle.

Approximately 7%–10% of the general human population is allergic to penicillin and related drugs (Dayan, 1993). The animal-derived products containing violative penicillin residues may cause severe allergic response to consumers. There is sufficient evidence that consumption of beef or pork products containing violative penicillin residues can cause anaphylactic reactions (Dayan, 1993; Gomes and Demoly, 2005; Raison-Peyron et al., 2001). Starting in 2017, the US Food and Drug Administration (US FDA) has ended the use of any medically important antibiotics, including penicillin G, for growth-promotion purposes in all food animals, and increases the oversight of veterinarians for all other antibiotic uses as animal drugs (FDA, 2015, 2016a). The guidance is based on US FDA's concerns for the development of antibiotic resistance to human and animal bacterial pathogens when antibiotics are used in food-producing animals in an injudicious way (FDA, 2013a). Therefore, the establishment of scientific tools to prevent violative penicillin G residues and to improve food safety is required.

Physiologically based pharmacokinetic (PBPK) models are mechanism-based models that incorporate physiological and chemical-specific parameters to simulate the absorption, distribution, metabolism and elimination of chemicals in the body using mathematical equations (Andersen, 2003; Lin et al., 2016a; WHO, 2010). PBPK models can be used to predict tissue residues and extralabel WDIs of veterinary drugs. Multiple PBPK models have been developed for a variety of veterinary drugs, including cyadox (Huang et al., 2015; Yang et al., 2015c), danofloxacin (Yang et al., 2015a), doxycycline (Yang et al., 2012), enrofloxacin (Lin et al., 2016b), florfenicol (Yang et al., 2013), flunixin (Leavens et al., 2014), marbofloxacin (Yang et al., 2014b), melamine (Buur et al., 2008), midazolam (Cortright et al., 2009), olaquindox (Yang et al., 2014a), oxytetracycline (Brocklebank et al., 1997; Craigmill, 2003; Lin et al., 2015), quinocetone (Zhu et al., 2017), sulfamethazine (Buur et al., 2006, 2005, 2009), tulathromycin (Leavens et al., 2012), and valnemulin (Yuan et al., 2011). However, there is no PBPK model of penicillin G available in food-producing animals.

We previously developed a mixed-effect population pharmacokinetic (popPK) model of penicillin G in cattle and swine (Li et al., 2014), but popPK modeling is not a physiologically based mechanistic approach and thus is limited in usefulness to extrapolate to other scenarios (i.e., to different routes and species). Therefore, the objective of this study was to develop a PBPK model for predicting tissue residues and estimate extended WDIs of penicillin G in swine and cattle treated with extralabel doses. In the present study, the term withdrawal period refers to the time needed for tissue residue

concentrations to decrease below tolerances determined using the 99th percentile tolerance limit method with a 95% confidence based on FDA guidance (FDA, 2016b), whereas WDI (withdrawal interval) is used to refer to the time estimated using other methods, such as the population PBPK model.

2. Methods

2.1. Data source for model calibration

The Food Animal Residue Avoidance Databank (FARAD) comparative pharmacokinetic database, an initiative supported by USDA to mitigate unsafe chemical residues in animal-derived products, was used as the primary source of data to calibrate and evaluate swine and cattle model (Craigmill et al., 2006; Riviere et al., 1986, 2017). Pharmacokinetic data in cattle and swine after IM or SC administration of procaine penicillin G were selected. Key information and a brief description of selected studies is shown in Table 1. Time-concentration data were extracted from graphs of selected pharmacokinetic studies using WebPlotDigitizer (version 3.10, <http://arohatgi.info/WebPlotDigitizer>), the web based tool for extracting data from plots and images.

2.2. Model structure

The PBPK model consisted of seven compartments corresponding to different tissues in the body, including liver, kidney, muscle, fat, lung, and the rest of body connected by the circulating blood system (Fig. 1). For food safety purposes, all the major edible tissues, including liver, kidney, muscle, and fat, were included. The lung was also included as a compartment as it is the therapeutic target tissue for penicillin G. Each compartment was defined by a tissue weight and tissue blood flow rate. The flow-limited model, which performed well for veterinary drugs with small molecular weights, was applied in the current model. Berkeley Madonna (Version 8.3.23.0; University of California at Berkeley, CA, USA) was used to develop the model and run all simulations. The model code is provided in the Supplementary Materials and is also available from our website (<http://iccm.k-state.edu/>). Only key or new mathematical equations are described in detail below.

As IM and SC injections are the labeled routes of administrations for penicillin G, they were incorporated into this model. Based on the previous studies, the rate-limiting step of absorption is the hydrolysis of penicillin from the procaine moiety (KuKanich et al., 2005; Uboh et al., 2000). The undissolved procaine penicillin G acts as the depot of penicillin G, and maintains the therapeutic concentration of penicillin G for at least 24 h (Papich and Riviere, 2009; Uboh et al., 2000). The IM and SC injections were simulated using a two-compartment injection site model with a dissolution process based on the approach used to simulate intramuscular absorption of long-acting oxytetracycline (Lin et al., 2015, 2017). This approach divides penicillin G into dissolved penicillin G moieties and undissolved procaine penicillin G acting as depot (Fig. 1). The related equations describing IM and SC absorption of penicillin G are available in Supplementary Materials (Equations (S1)–(S7)).

The multiple doses of IM and SC injections are the commonly used therapeutic scenarios for procaine penicillin G in swine and cattle. The 'PULSE' function was used for repeated administrations of chemicals in PBPK models coded in acslX (Lin et al., 2013; Poet et al., 2016). However, the 'PULSE' function is defined slightly different in Berkeley Madonna from other programming languages. It is not a rectangular pulse function, but a triangular function which specifies the input as an isosceles triangle with a base that is the length of two integration time steps (Krause and Lowe, 2014;

Table 1

Summary of pharmacokinetic studies of penicillin G in swine and cattle used for calibration and evaluation of the PBPK model.

Species/purpose	Route	Dose (mg/kg)	Repeat dose	Sex	n	Age (week)	BW (kg)	Matrix	Assay	Ref.
<i>Swine Calibration</i>										
<i>Evaluation</i>	IM, SC	15.5, 11.7	1	NA	9	2	3.3, 3.6	P	LCMS	Ranheim et al., 2002
	IM	15, 65	3,5	Both	6	21	100	L, K, M, F, P	HPLC	Korsrud et al., 1998
<i>Cattle Calibration</i>	IM	15	3	Both	6	21	100	K, M, P	HPLC	Korsrud et al., 1996
	IM, SC	24, 65 (IM); 65 (SC)	5 (IM) 1 (SC)	Male	3	NA	480	P	HPLC	Papich et al., 1993
<i>Evaluation</i>	IM	24, 65	5	Male	3	NA	485	L, K, M, P	HPLC	Korsrud et al., 1993
	SC	7.4	1	NA	3	28	93	P	Agar Diffusion Test	Trolldenier et al., 1986
	IM	7	3	Male	3	48	262	K, P	LCMSMS	Chiesa et al., 2006

Notes: The abbreviations for route: IM, intramuscular injection; SC, subcutaneous injection. The abbreviations for matrix: P, plasma; L, liver; K, kidney; M, muscle; F, fat. The abbreviations for assay: LCMS, liquid chromatography mass spectrometry; HPLC, high performance liquid chromatography; LCMSMS, liquid chromatography tandem mass spectrometry. NA: not available.

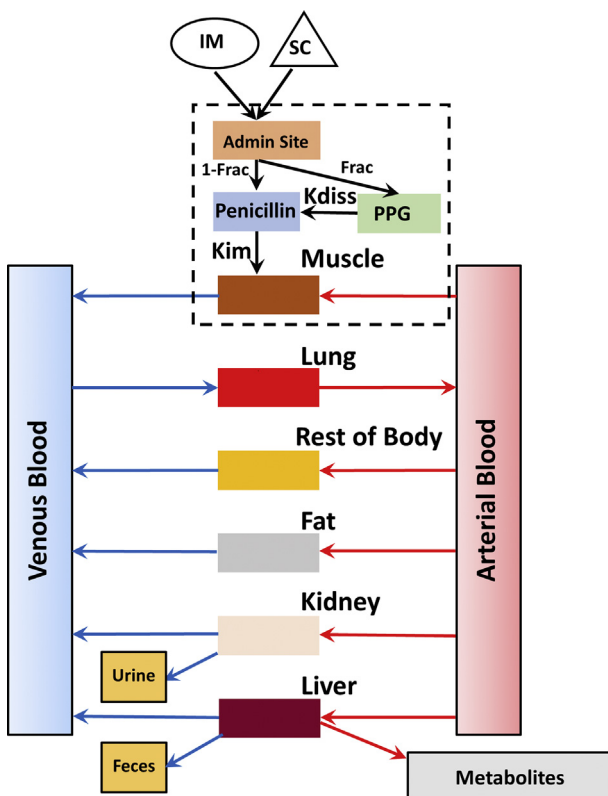


Fig. 1. A schematic diagram of the physiologically based pharmacokinetic (PBPK) model for penicillin G in swine and cattle. Two different administration routes including intramuscular (IM) and subcutaneous (SC) injections are presented in the model. A mechanistic two-compartment dissolution model is used to describe the IM and SC injections of procaine penicillin G (PPG). Admin Site represents administration site. (For interpretation of the references to colour in this figure legend, the reader is referred to the web version of this article.)

Macey et al., 2009). As the integration step is always in a small number, the function adds the amount of drugs almost instantaneously, which can well simulate the process of an injection. The multiple-dose scenario was achieved by using the conditional operator of 'IF ... THEN ... ELSE ...' to create a control factor. If the time surpasses the multiple dose period, 0 will be assigned to the control factor. Then no further input dose will be accounted into the model. The equations for multiple-dose IM injection are listed below as an example (Equation (1) and Equation (2)):

$$Rinput = \text{PULSE}(\text{Dose}, \text{StartTime}, \text{DoseInterval}) * Tdosingperiod \quad (1)$$

$$Tdosingperiod = \begin{cases} \text{if time} < \text{Tdoses} * \text{DoseInterval} \\ \quad - \text{DT} \text{ then 1 else 0} \end{cases} \quad (2)$$

where Dose is the dose of IM injection (mg); StartTime is the time to start IM administration (hour), and 0 was used in this model; DoseInterval is the time of each dosing interval (hour); Tdosingperiod represents the control factor for multiple injections (unitless); Tdoses is the times of multiple dosing (unitless); DT is integration time step (hour), and default value is 0.02 in Runge-Kutta 4 method. One DT was added to exposure time, when PULSE equation was used. This modeling approach can be extrapolated to simulate different exposure scenarios by modifying Dose, StartTime, DoseInterval, Tdosingperiod, and Tdoses.

Penicillin was reported to be metabolized in humans to penicilloic acids and 6-aminopenicillanic acid (6-APA), and the ratio of metabolites to penicillin G in human urine is 19% after IM injection (Cole et al., 1973). Penicilloic acid, the inactive metabolite, represents about 16–30% of an intramuscular dose of penicillin G from DrugBank (DrugBank, 2016; Wishart et al., 2006). Unlike in humans, the metabolism of penicillin G in food-producing animals is not well known, so a simplified first-order metabolic rate was used to simulate hepatic metabolism in this model (Fisher, 2000; Krishnan et al., 2009). Equation (S8) describing the process of first-order liver metabolism (Supplementary Materials). Penicillin G is reported mainly excreted via urine in mammals (Tsuji et al., 1983), a first-order urinary elimination rate in the kidney compartment was adapted from previous research (Craigmill, 2003). Equation (S9) describing the process of first-order urinary elimination is available in the Supplementary Materials. The rate of change for penicillin G in each tissue compartment was described using mass balance differential equations as we previously described (Leavens et al., 2012; Lin et al., 2015). Only penicillin G not bound to plasma proteins was considered as available for distribution. Equation (S10)–(S11) describe the mass balance of penicillin G in flow-limited compartments using kidney as an example (Supplementary Materials).

2.3. Model parameterization

The PBPK models are composed of two different types of parameters including species-specific physiological parameters and

chemical-specific parameters. To the extent possible, physiological parameters were collected from the original literature where these parameters were measured experimentally. In swine, the mean body weight (BW), cardiac output (QCC), tissue volume fractions of liver (VLC), kidneys (VKC), muscle (VMC), and fat (VFC), as well as the fractions of blood flows to kidneys (QKC) and muscle (QMC) were directly from or calculated based on published experimental data (Armstrong et al., 1987; Doornenbal et al., 1986; Hannon et al., 1990; Lundein et al., 1983; Phuc and Hieu, 1993; Tranquilli et al., 1982). In cattle, the mean body weight, cardiac output, and tissue volume fractions of liver, kidneys, and lung (VLuC), as well as the fraction of blood flow to liver (QLC) were directly from or calculated based on the experimental data (Doyle et al., 1960; Lescoat et al., 1996; Mirzaei et al., 2011; Swett WW et al., 1933). The values for other physiological parameters in swine and cattle were adapted from previous PBPK models (Leavens et al., 2014; Lin et al., 2016b; Upton, 2008). All physiological parameters are summarized in Tables 2 and 3. As for chemical-specific parameters (e.g., partition coefficients) of penicillin G, the original values were adapted from the previous PBPK models of penicillin G in the rat (Cao and Jusko, 2012; Tsuji et al., 1979, 1983), and protein binding parameters were adapted from experimental data measured in swine and cattle (Keen, 1965). These parameter values were used as initial values in the model calibration, adjusted using the Curve Fitting module in Berkeley Madonna, and further optimized as needed by visually fitting model simulations to observed pharmacokinetic data of penicillin G. Values of all chemical-specific parameters for penicillin G in swine and cattle models are provided in Tables 2 and 3.

2.4. Model evaluation: validation and sensitivity analysis

The performance of the PBPK model was evaluated by comparing model simulations with experimental plasma and tissue data not used in the model parameterization as listed in Table 1. On the basis of World Health Organization (WHO) guidelines (WHO, 2010), if the simulations matched the measured kinetic profiles and were generally within a factor of two of the measured values, the model was considered reasonable and validated. These criteria are based on the considerations that calibration data sets and evaluation data sets are obtained under different conditions (e.g., different experimental animals/human subjects, laboratories, and detection methods), so some level of discordance is to be expected (WHO, 2010). The goodness of fit between log-transformed values of observed and predicted plasma and tissue concentrations were further analyzed with linear regression and the determination coefficient (R^2) was calculated.

A local sensitivity analysis was performed to determine which parameters were most influential on the 24-hour AUC of plasma, liver, kidney, and muscle concentrations of penicillin G. Each parameter was increased by 1%, 5% and 10%, and the corresponding 24-hour AUC of penicillin concentrations were computed. Normalized sensitivity coefficient (NSC) was calculated using Equation (S12) (Lin et al., 2011; Mirfazaelian et al., 2006) provided in Supplementary Materials. The relative influence of each parameter on the response variables was categorized as: low: $|NSC| < 0.2$; medium: $0.2 \leq |NSC| < 0.5$; high: $0.5 \leq |NSC|$ (Lin et al., 2013; Yoon et al., 2009).

Table 2
Values and distributions of parameters used in the Monte Carlo analysis for the swine model.

Parameter	Abbreviation	Distribution	Mean	SD	CV	Lower bound	Upper bound	Reference
Body weight (kg)	BW	Normal	33.182	6.451E+00	0.194 [#]	20.539	45.825	[1–4]
Cardiac output (L/h/kg)	QCC	Normal	8.543	1.910E+00	0.224 [#]	4.800	12.287	[1, 2]
Tissue volume (fraction of body weight, unitless)								
Arterial blood	VartC	Normal	0.016	4.680E-03	0.300	0.006	0.025	[5]
Venous blood	VvenC	Normal	0.044	1.332E-02	0.300	0.018	0.071	[5]
Liver	VLC	Normal	0.023	3.609E-04	0.015 [#]	0.023	0.024	[2, 3, 6]
Kidney	VKC	Normal	0.005	1.738E-04	0.038 [#]	0.004	0.005	[2, 3]
Muscle	VMC	Normal	0.355	2.494E-03	0.007 [#]	0.351	0.360	[7]
Fat	VFC	Normal	0.235	1.802E-02	0.077 [#]	0.200	0.270	[4]
Lung	VLuC	Normal	0.010	3.000E-03	0.300	0.004	0.016	[5]
Rest of body	VrestC	Normal	0.312	9.346E-02	0.300	0.128	0.495	Total adds to 1
Blood flow (fraction of cardiac output, unitless)								
Liver	QLC	Normal	0.273	8.175E-02	0.300	0.112	0.433	[5, 8]
Kidney	QKC	Normal	0.116	1.733E-02	0.149 [#]	0.082	0.150	[1, 2]
Muscle	QMC	Normal	0.293	4.216E-02	0.144 [#]	0.211	0.376	[3]
Fat	QFC	Normal	0.128	3.825E-02	0.300	0.053	0.202	[5, 8]
Rest of body	QrestC	Normal	0.190	5.712E-02	0.300	0.078	0.302	Total adds to 1
Absorption rate constant (/h)								
Intramuscular	Kim	Lognormal	0.070	2.100E-02	0.300	0.038	0.119	Model fitted
	Frac	Lognormal	0.010	1.000E-03	0.100	0.008	0.012	Model fitted
	Kdiss	Lognormal	0.007	2.100E-03	0.300	0.004	0.012	Model fitted
Subcutaneous	Ksc	Lognormal	0.250	7.500E-02	0.300	0.135	0.426	Model fitted
	Fracsc	Lognormal	0.500	5.000E-02	0.100	0.409	0.605	Model fitted
	Kdisscc	Lognormal	0.005	1.500E-03	0.300	0.003	0.009	Model fitted
Tissue:plasma partition coefficient for the parent drug (unitless)								
Liver	PL	Lognormal	0.080	1.600E-02	0.200	0.053	0.116	Model fitted
Kidney	PK	Lognormal	7.000	1.400E+00	0.200	4.656	10.119	Model fitted
Muscle	PM	Lognormal	0.150	3.000E-02	0.200	0.100	0.217	Model fitted
Fat	PF	Lognormal	0.035	7.000E-03	0.200	0.023	0.051	Model fitted
Lung	PLu	Lognormal	0.180	3.600E-02	0.200	0.120	0.260	[9]
Rest of body	Prest	Lognormal	0.479	9.580E-02	0.200	0.319	0.692	[10]
Hepatic metabolic rate (/h/kg)	KmC	Lognormal	0.050	1.500E-02	0.300	0.027	0.085	Model fitted
Percentage of plasma protein binding (unitless)	PB	Lognormal	0.366	1.098E-01	0.300	0.197	0.623	[11]
Urinary elimination rate constant (L/h/kg)	KurineC	Lognormal	1.400	4.200E-01	0.300	0.754	2.384	Model fitted

Notes: Some parameters were estimated by fitting the PBPK model with the pharmacokinetic data. These parameters were marked as 'model fitted'. [1] Hannon et al., 1990; [2] Tranquilli et al., 1982; [3] Lundein et al., 1983; [4] Doornenbal et al., 1986; [5] Lin et al., 2016b; [6] Phuc and Hieu, 1993; [7] Armstrong et al., 1987; [8] Huang et al., 2015; [9] Tsuji et al., 1983; [10] Cao and Jusko, 2012; [11] Keen, 1965. A pound sign (#) indicates the CV was determined based on previous experimental data.

Table 3

Values and distributions of parameters used in the Monte Carlo analysis for the cattle model.

Parameter	Abbreviation	Distribution	Mean	SD	CV	Lower bound	Upper bound	Reference
Body weight (kg)	BW	Normal	299.957	4.618E+01	0.154 [#]	209.450	390.464	[1]
Cardiac output (L/h/kg)	QCC	Normal	5.970	1.990E+00	0.333 [#]	2.070	9.870	[2]
Tissue volume (fraction of body weight, unitless)								
Arterial blood	VartC	Normal	0.010	3.120E-03	0.300	0.004	0.017	[3]
Venous blood	VvenC	Normal	0.030	8.880E-03	0.300	0.012	0.047	[3]
Liver	VLC	Normal	0.014	1.630E-03	0.120 [#]	0.010	0.017	[4]
Kidney	VKC	Normal	0.002	4.321E-04	0.174 [#]	0.002	0.003	[4]
Muscle	VMC	Normal	0.270	8.100E-02	0.300	0.111	0.429	[3, 5]
Fat	VFC	Normal	0.150	4.500E-02	0.300	0.062	0.238	[3, 5]
Lung	VLuC	Normal	0.008	1.696E-03	0.212 [#]	0.005	0.011	[3–5]
Rest of body	VrestC	Normal	0.516	1.548E-01	0.300	0.213	0.819	Total adds to 1
Blood flow (fraction of cardiac output, unitless)								
Liver	QLC	Normal	0.405	1.942E-01	0.480 [#]	0.024	0.785	[2, 6]
Kidney	QKC	Normal	0.090	2.700E-02	0.300	0.037	0.143	[3]
Muscle	QMC	Normal	0.180	5.400E-02	0.300	0.074	0.286	[3]
Fat	QFC	Normal	0.080	2.400E-02	0.300	0.033	0.127	[3]
Rest of body	QrestC	Normal	0.245	7.360E-02	0.300	0.101	0.390	Total adds to 1
Absorption rate constant (/h)								
Intramuscular	Kim	Lognormal	0.070	2.100E-02	0.300	0.038	0.119	Model fitted
	Frac	Lognormal	0.600	1.800E-01	0.100	0.491	0.726	Model fitted
	Kdiss	Lognormal	1.000E-05	3.000E-06	0.300	5.388E-06	1.703E-05	Model fitted
Subcutaneous	Ksc	Lognormal	0.020	6.000E-03	0.300	0.011	0.034	Model fitted
	Fracsc	Lognormal	0.700	2.100E-01	0.100	0.573	0.847	Model fitted
	Kdisscc	Lognormal	1.000E-04	3.000E-05	0.300	5.388E-05	1.703E-04	Model fitted
Tissue:plasma partition coefficient for the parent drug (unitless)								
Liver	PL	Lognormal	3.000	6.000E-01	0.200	1.995	4.337	Model fitted
Kidney	PK	Lognormal	2.500	5.000E-01	0.200	1.663	3.614	Model fitted
Muscle	PM	Lognormal	0.300	6.000E-02	0.200	0.200	0.434	Model fitted
Fat	PF	Lognormal	0.040	8.000E-03	0.200	0.027	0.058	Model fitted
Lung	PLu	Lognormal	0.180	3.600E-02	0.200	0.120	0.260	[7]
Rest of body	Prest	Lognormal	0.479	9.580E-02	0.200	0.319	0.692	[8]
Hepatic metabolic rate (/h/kg)	KmC	Lognormal	0.0025	7.500E-04	0.300	0.001	0.004	Model fitted
Percentage of plasma protein binding (unitless)	PB	Lognormal	0.483	1.449E-01	0.300	0.260	0.822	[9]
Urinary elimination rate constant (L/h/kg)	KurineC	Lognormal	0.450	1.350E-01	0.300	0.242	0.766	Model fitted

Notes: Some parameters were estimated by fitting the PBPK model with the pharmacokinetic data. These parameters were marked as 'model fitted'. [1] Mirzaei et al., 2011; [2] Doyle et al., 1960; [3] Lin et al., 2016b; [4] Swett WW et al., 1933; [5] Leavens et al., 2014; [6] Lescoat et al., 1996; [7] Tsuji et al., 1983; [8] Cao and Jusko, 2012; [9] Keen, 1965. A pound sign (#) indicates the CV was calculated based on previous experimental data.

2.5. Monte carlo analysis

Monte Carlo simulation is used to obtain numerical results based on repeated random sampling of parameter values from specified probability functions for each parameter. This method is widely employed in mathematical models to study population characteristics in biomedical problems (Kerr et al., 2008; Shi et al., 2016), including PBPK models to estimate tissue residues and withdrawal intervals (Buur et al., 2006; Yang et al., 2012). In current PBPK modeling, Monte Carlo simulation was also applied to estimate the effects of parameter uncertainty and intra-species variability of swine and cattle on model simulations. One-thousand iterations (the maximum number of iterations in a batch run in Berkeley Madonna) were carried out for each Monte Carlo analysis. For these simulations, hypothetical populations of swine and cattle, respectively, with all physiological and chemical-specific parameters distributed randomly around the mean values were specified in Tables 2 and 3, respectively. Log-normal distributions of model parameters were assumed for all chemical-specific parameters such as partition coefficients, absorption rate constants, elimination rate constants, etc. Physiological parameters, including body weights, cardiac outputs, and fractions of blood flows and tissue volumes were assumed to be normally distributed (Clewell et al., 2000; Shankaran et al., 2013; Sterner et al., 2013; Tan et al., 2006; Yang et al., 2015b).

Model parameters were varied randomly around the values (central tendencies) used or estimated in model calibration. Probabilistic distributions (variability) of model parameter values were derived from previous experimental data. To make the optimal use

of experimental data in livestock, an extensive literature search was carried out for physiological parameters of swine and cattle including blood flows and tissue volumes. For physiological parameters in swine, coefficients of variability (CVs) of the body weight, the cardiac output, the tissue volume fractions of liver, kidneys, muscle, and fat, and the fractions of blood flows in kidneys and muscle were calculated from previous experimental data, which were the same data as those used for calculation of means (Armstrong et al., 1987; Doornenbal et al., 1986; Hannon et al., 1990; Lundein et al., 1983; Phuc and Hieu, 1993; Tranquilli et al., 1982). CVs of the body weight, the cardiac output, and the tissue volume fractions of liver, kidneys, and lung, and the fractions of blood flows in liver for cattle were calculated based on the experimental data (Doyle et al., 1960; Lescoat et al., 1996; Mirzaei et al., 2011; Swett WW et al., 1933). For other physiological parameters of which no experimental data were available and for the chemical-specific parameters, their CVs were assigned as 10% for undissolved fractions of penicillin G (Frac), 20% for partition coefficients and 30% for physiological parameters, absorption, and elimination rate constants based on the default assumptions used in other PBPK models (Clewell and Clewell, 2008; Henri et al., 2016; Yang et al., 2015b, 2016). To ensure the randomly selected parameters biologically plausible, the 2.5th and 97.5th percentiles of each parameter were calculated as the upper and lower bounds and listed in Tables 2 and 3.

As all the physiological parameters were randomly chosen based on their distributions, the sum of tissue volumes or the sum of fractions of blood flows may be larger or smaller than 1. It is necessary to use adjustment factors to ensure the plausibility and

mass balance for the PBPK model (Covington et al., 2007; Gelman et al., 1996; Sterner et al., 2013). The Monte Carlo model was set up to batch run for 1000 times with model parameters randomly selected from the defined distributions.

$$\mu_{lnx} = \ln \left(\frac{\mu_x^2}{\sqrt{\sigma_x^2 + \mu_x^2}} \right) \quad (3)$$

$$\sigma_{lnx} = \sqrt{\ln \left(1 + \frac{\sigma_x^2}{\mu_x^2} \right)} \quad (4)$$

$$\text{Lognormal}(\mu_x, \sigma_x) = \exp(\text{Normal}(\mu_{lnx}, \sigma_{lnx})) \quad (5)$$

where μ_x is the mean for lognormal distribution; σ_x is the standard deviation for lognormal distribution; μ_{lnx} is the mean after the transformation to normal distribution; σ_{lnx} is the standard deviation after the transformation to normal distribution.

The 'Equation Help' in Berkeley Madonna (Version 8.3.23.0) defines 'NORMAL' function requiring the mean and the variance to establish the random numbers. This statement for 'NORMAL' function in Berkeley Madonna is not correct. After extensive simulations, we found that the 'NORMAL' function in Berkeley Madonna actually requires inputs of the mean and standard deviation of the defined normal distribution, which is the same as the corresponding function in R language and MATLAB. Some of the model parameters are in the lognormal distributions. However, the lognormal function is not available in Berkeley Madonna. As the lognormal distribution is a continuous probability distribution of a random variable whose logarithm is normally distributed, the inverse natural logarithmic transformation of the 'NORMAL' function can be used to produce lognormally distributed random numbers (Equation (5)). To use Equation (5), the mean and the standard deviation in lognormal distribution should be transformed into model parameters in normal distribution (Equations (3) and (4)) (Gujer, 2008a).

In addition, the 'NORMAL' function establishes random numbers at each integration time step (DT) in the PBPK model. The 'NORMAL' function will assign different random numbers for selected parameters at each time step, not one constant random value for each run. To avoid this issue, the initialization equation 'INIT' was applied to generate randomly selected number for parameters. Then the 'NEXT' equation was used to assign the randomly selected value in 'INIT' function to each of specific parameters. The pair of 'INIT' and 'NEXT' functions help to ensure each of the parameters assigned only one constant value in each run (Gujer, 2008b). Furthermore, the 'LIMIT' function was used to make sure the random numbers fell in the range between the lower and upper bounds for each of the parameters.

Three different therapeutic scenarios were analyzed using Monte Carlo simulations for both swine and cattle. The label dose 6000 IU/kg (6.5 mg/kg), and two commonly used extralabel doses ($5 \times$ label dose, 32.5 mg/kg; $10 \times$ label dose, 65 mg/kg) were simulated for 5 repeated IM injections with 24-hour intervals. Each of the simulations was run for 1000 times. The median, 1th and 99th percentiles of simulated results were calculated and plotted without confidence intervals.

2.6. Withdrawal interval estimation

The extralabel WDIs were determined using the present PBPK models based on results of the Monte Carlo simulation. The extralabel WDI for cattle was determined when the values of 99th

percentiles of tissue residues depleted to fall below the tolerance. The tolerance of penicillin G for edible tissues in cattle is 0.05 µg/g established by US FDA (Brynes, 2005). In the US, the Food Safety and Inspection Service (FSIS) has established an action limit of 25 ng/g for penicillin residues detected in swine tissues (FSIS, 2013). By using more sensitive LC-MS/MS method, the LOD of penicillin G in kidney is 1.8 ng/g, in muscle is 0.7 ng/g, and in serum is 1.5 ng/g (Apley et al., 2009; Lupton et al., 2014). The LOD in liver tissue was assumed the same as the LOD in kidney of swine. As there is zero-tolerance limit for penicillin G in edible tissues in swine (Brynes, 2005), the extralabel WDI for swine was determined when the values of 99th percentiles of tissue residues depleted to below FSIS action limit or LOD.

3. Results

3.1. Model calibration

Model predictions of concentrations of penicillin G in plasma and edible tissues at different time points after administration were compared with observed concentrations in pigs exposed to penicillin G through repeated IM dose of 15 mg/kg for three times, repeated IM dose of 65 mg/kg for 5 times, and single SC dose of 11.7 mg/kg (representative results are shown in Fig. 2; other results are provided in Fig. S1). Overall, the model well simulated the kinetic profiles of penicillin G in different edible tissues and plasma in swine. For the repeated dose scenarios, at the later time points the model can accurately predict the tissue residues in plasma and kidney (Fig. 2), which are important for residue monitoring and the determination of times when concentrations of tissue residues fall below or near tolerance or LOD for penicillin G.

After extrapolating this PBPK model from swine to cattle, the predicted results of penicillin G concentrations in plasma and liver after 5 IM repeated injections with two different doses correlated with the observed data (Fig. 3). Similar to the swine model, the model for cattle accurately simulated the terminal phase of penicillin G in edible tissues with 5 repeated IM injections (Fig. 3B, D). Even for concentrations of tissue residues lower than tolerance, the model predictions of penicillin G concentrations were in good agreement with observed data after IM injections (Fig. 3B, D). The other results of model calibrations in cattle are shown in Fig. S2. Overall, the predictions of current PBPK model of penicillin G well capture the kinetic profile observed in pharmacokinetic studies in cattle.

3.2. Model evaluation

Measured concentrations of penicillin G in edible tissues of swine after IM injections of 15 mg/kg for 3 consecutive days were compared with model predictions (Fig. 4A B and C). Overall, the model predicted the concentrations of penicillin G adequately at different time points (within 2-fold). For the cattle model, the evaluation results shown in panels A, B, and C of Fig. 5 indicate the simulated concentrations are consistent with the measured results from different studies. The goodness of fit was evaluated using the determination coefficient (R^2). The value of R^2 between log-transformed values of measured and simulated concentrations of penicillin G in edible tissues and plasma was 0.89 for PBPK model in swine (Fig. 4D). In the pharmacokinetic data used for swine model evaluation, there were only two data points available for muscle and three for plasma that were not sufficient for regression analysis for individual tissue data, so all data were pooled together for overall regression analysis. The R^2 represents an indicator of the overall model simulation performance. For the PBPK model in cattle, the value of overall R^2 was 0.91 (Fig. 5D). The R^2 for data in

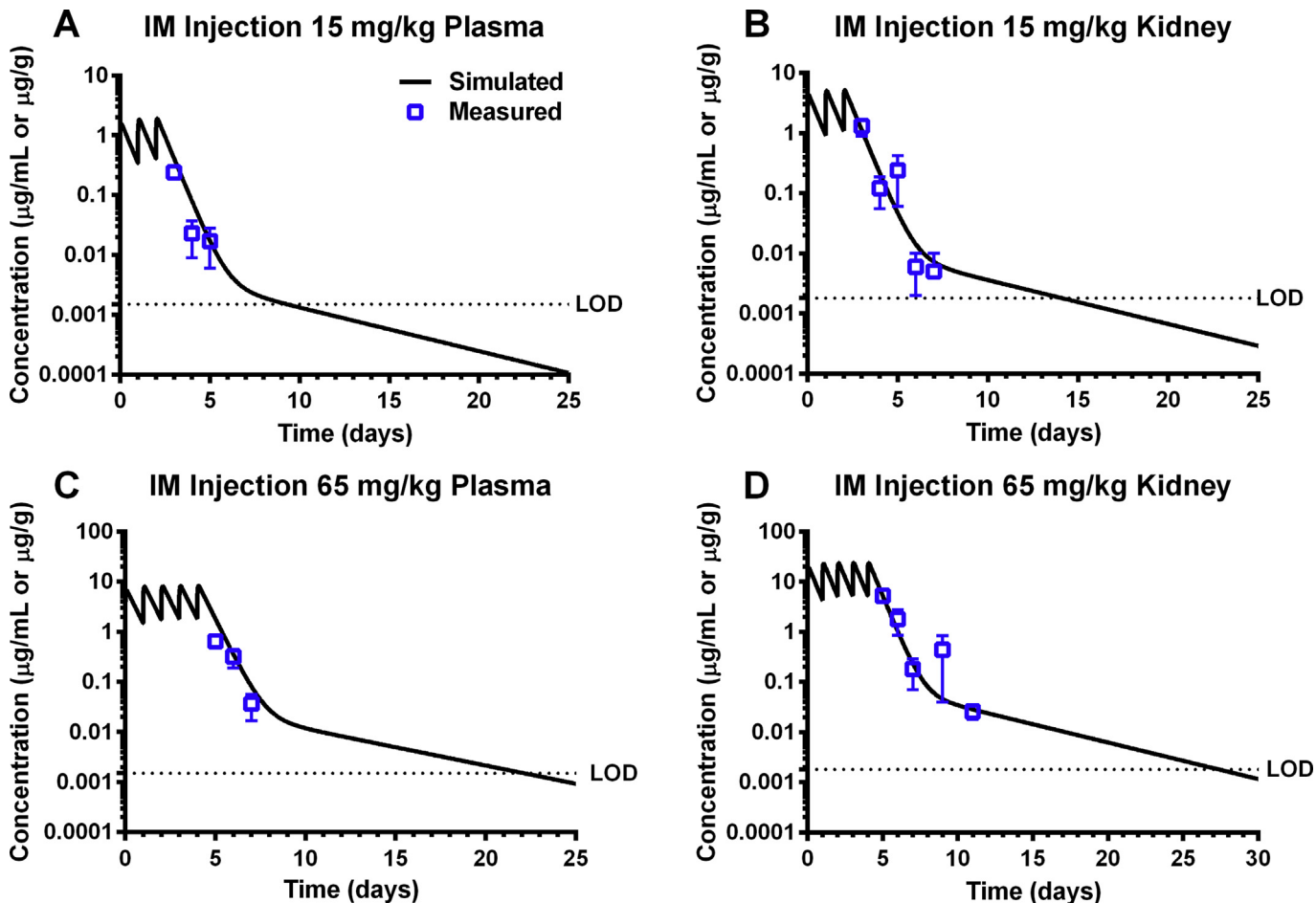


Fig. 2. Calibration of the swine model. Comparison of model predictions (solid line) and observed data (blue squares) for concentrations of penicillin G in the plasma and kidneys of swine exposed to procaine penicillin G via repeated 3 doses of IM injections (15 mg/kg, A, B) and repeated 5 doses of IM injections (65 mg/kg, C, D). Experimental data (mean \pm SEM) are from the study of Korsrud et al. (1998). The limit of detection (LOD) is shown on each panel using dotted line. LOD for the kidney is 1.8 ng/g, and for the plasma is 1.5 ng/g (Lupton et al., 2014). (For interpretation of the references to colour in this figure legend, the reader is referred to the web version of this article.)

kidney was 0.96, and for plasma was 0.88. The relatively lower R^2 for plasma was due to the overestimation for some of the data points in plasma (within two-fold difference). Overall, the PBPK model adequately simulates the measured results in relevant edible tissues from independent studies for both swine and cattle.

3.3. Parameter sensitivity

The local sensitivity analysis was carried out for twenty-nine model parameters based on PBPK model for swine. Results of the local sensitivity analysis based on 1% variation of the parameter values are shown in Table S1. Only parameters with at least one absolute value of NSC greater than 0.1 are shown in the table. The comparison of NSCs by sensitive parameters with 1%, 5% and 10% variations was plotted using a spider plot (Fig. S3). The results indicate that the NSCs for each parameter were not substantially different among different variations of the parameter value. The AUC of liver tissue was highly sensitive to hepatic metabolic rate constant and liver partition coefficient with NSC values of -0.12 and 0.88, respectively. The AUC of kidney tissues was highly sensitive to urine elimination rate constant and kidney partition coefficient with NSC values of -0.92 and 1.00, respectively. For SC injection, all AUCs of selected tissues were highly sensitive to the

absorption rate constant of subcutaneous injections (Ksc) with the NSC value as 0.79.

3.4. Monte carlo analysis and withdrawal interval estimation

Based on results of the PBPK simulation shown above, among all edible tissues, the concentration of penicillin G depleted the slowest in the kidney for swine and in the liver for cattle, so the kidney tissue residue depletion profiles for swine and the liver tissue residue depletion profiles for cattle were chosen to determine the WDIs. The Monte Carlo simulations showed that the WDIs after 5 repeated IM injections in swine were 6 days, 10 days, and 16 days at dose levels of 6.5, 32.5, and 65 mg/kg after the last injection based on FSIS action limit. If based on current LOD, the WDIs for swine were 18 days, 33 days and 41 days for dose levels of 6.5, 32.5, and 65 mg/kg. For cattle, the WDIs were 5 days, 7 days, and 10 days at dose levels of 6.5, 32.5, and 65 mg/kg after the last injection, respectively (Fig. 6). Note that if the estimated WDI was a fraction of a day, it was rounded up to the next whole day. The label withdrawal periods were obtained from the Veterinarian's Guide to Residue Avoidance Management (VetGRAM) of FARAD (Riviere et al., 2017), and they are highly dependent on specific formulations. As an example, the label withdrawal periods of procaine

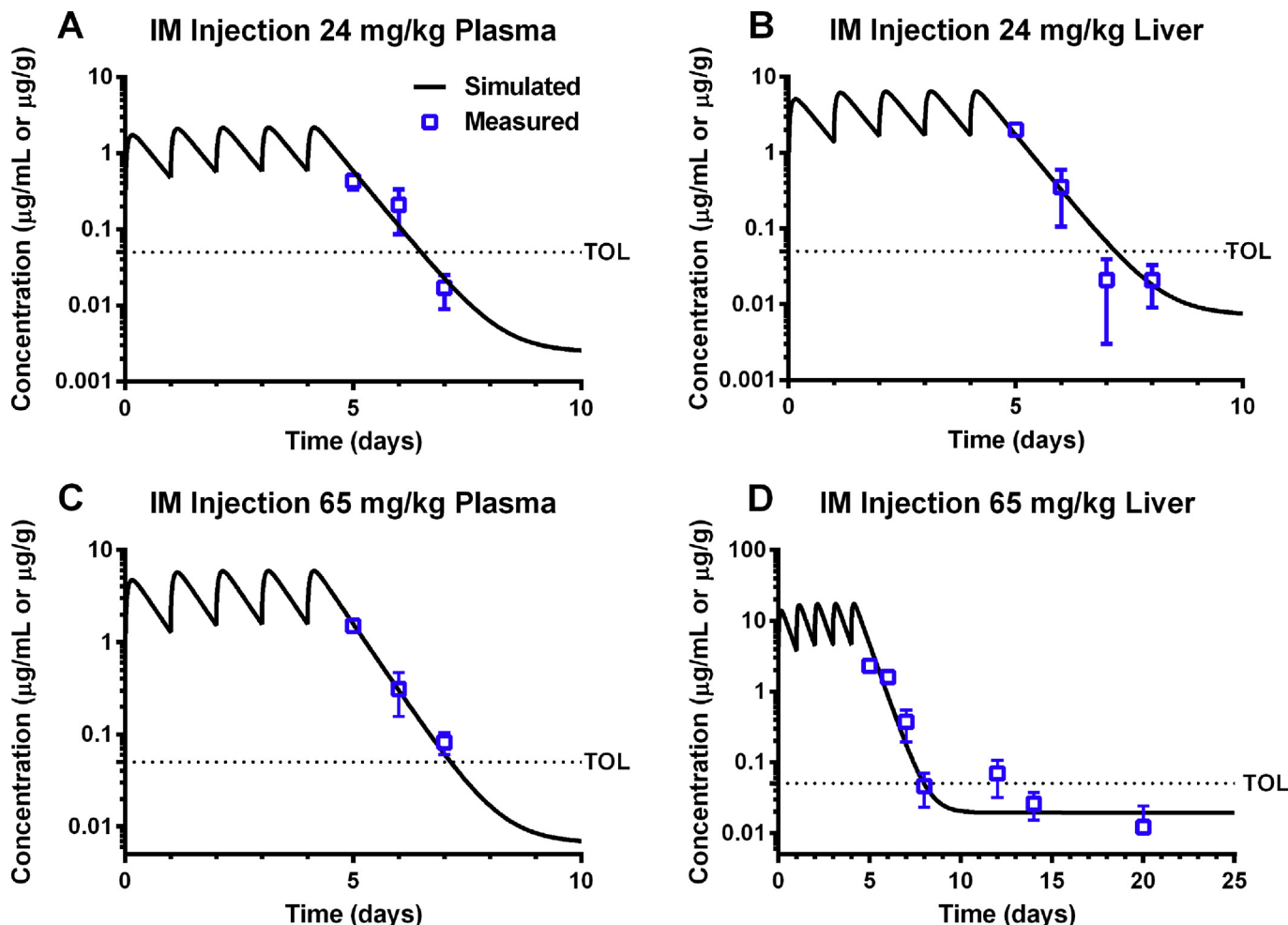


Fig. 3. Calibration of the cattle model. Comparison of model predictions (solid line) and observed data (blue squares) for penicillin G concentrations in the plasma and liver of cattle exposed to procaine penicillin G via IM repeated 5 doses at 24 mg/kg (A, B) and at 65 mg/kg (C, D) is shown. Experimental data (mean \pm SEM) are from the previous study by Korsrud et al. (1993). Tolerance (TOL) of penicillin G (0.05 $\mu\text{g/g}$) is shown on each of the panels using dotted line. (For interpretation of the references to colour in this figure legend, the reader is referred to the web version of this article.)

penicillin G (in NADA: 650–174) for swine is 6 days and for cattle is 4 days.

4. Discussion

A PBPK model was developed for procaine penicillin G through IM and SC administrations in swine and cattle, and then population simulation was applied to predict times needed for concentrations to fall below established tolerances for extralabel use of penicillin G. This is the first PBPK model of penicillin G used to predict the tissue residues and estimate extralabel WDIs in food-producing animals. The model well predicted tissue residues of penicillin G in edible tissues for both swine and cattle, and can be extrapolated to other food animal species. The population analysis was performed with Monte Carlo simulation technique considering the variances of all model parameters. The Monte Carlo analysis based on the PBPK model can help to estimate the extended WDIs for different extralabel use scenarios of penicillin G. The population PBPK model provides a useful tool to predict tissue residues of penicillin G in food-producing animals to aid food safety assessment.

The current PBPK model of penicillin G in swine and cattle has advantages over other pharmacokinetic models for penicillin G. A

minimal PBPK model with only two tissue compartments, which lumps compartments in whole-body PBPK model into compartments only with necessity (Nestorov et al., 1998), was applied for β -lactam antibiotics including penicillin G to estimate the clearance and steady-state volume (Cao and Jusko, 2012). However, for the PBPK model used in veterinary medicine for assessment of food safety, it is necessary to keep all the edible tissues as separate compartments in order to estimate individual tissue residues and WDIs. Recently, population mixed-effects pharmacokinetic models of penicillin G were developed to predict tissue residues and WDIs in swine and cattle (Li et al., 2014), and to optimize the dosage regimen in patients with infective endocarditis (Komatsu et al., 2016). Population pharmacokinetic modeling, which combines available pharmacokinetic data to make a population inference, is a useful approach in the area of food safety and veterinary medicine (Li et al., 2015; Martin-Jimenez and Riviere, 1998). However, compared to a PBPK model, the population pharmacokinetic model is not a physiologically based mechanistic method, which limits the extrapolation of the model beyond the inference range of experimental data (Lin et al., 2016a).

Compared to traditional pharmacokinetic and population pharmacokinetic models, PBPK models have unique advantages in predicting tissue residues and WDIs for veterinary medicines (Lin

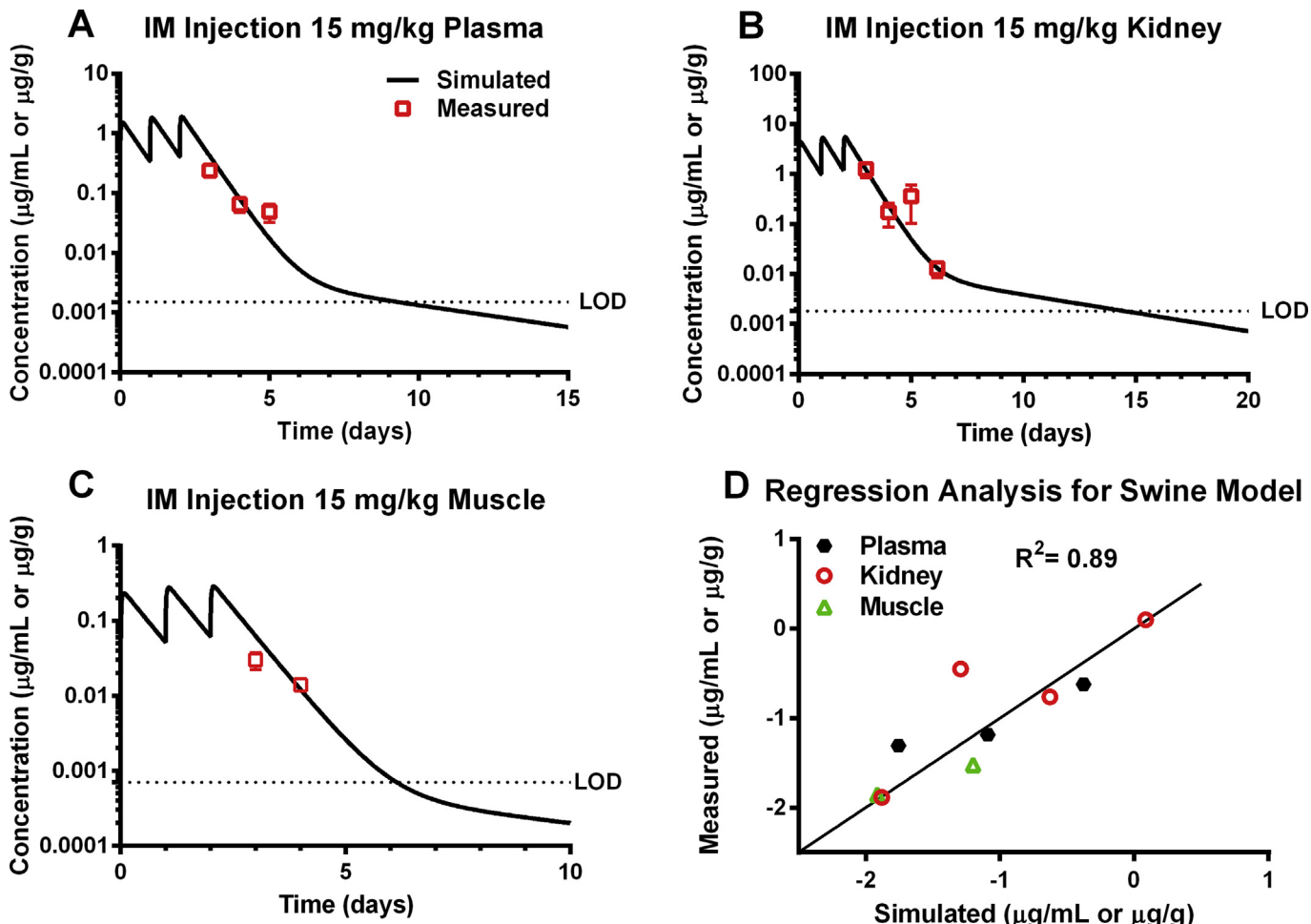


Fig. 4. Evaluation and regression analysis of the swine model. Comparison of model predictions (solid line) and observed data (red squares) for concentrations of penicillin G in the plasma, kidney, and muscle of pigs exposed to procaine penicillin G via IM injection for repeated 3 doses (15 mg/kg, A, B, C) is shown. Experimental data for A, B, C (mean \pm SEM) are from the study of Korsrud et al. (1996). Limit of detection (LOD) is shown on each of the three panels using dotted line. LOD for the plasma is 1.5 ng/g, for the kidney is 1.8 ng/g, and for the muscle is 0.7 ng/g (Lupton et al., 2014). Panel D represents the result of a regression analysis between log-transformed values of model-simulated and measured penicillin G concentrations for swine model. R^2 value and the regression line are shown in the panel. (For interpretation of the references to colour in this figure legend, the reader is referred to the web version of this article.)

et al., 2016a). PBPK models are based on the physiological considerations of modeled drugs and all model compartments are physiologically realistic, and population variability in physiological parameters within each compartment can be estimated. Thus, the model can help predict the concentrations of drug residues in a specific tissue of interest following different therapeutic scenarios. This is important because for its application in veterinary medicine and food safety, the concentrations of drug residues in tissues help to determine the WDIs. The other advantage of a PBPK model is that newly available data related to drug absorption, distribution, metabolism and excretion can be directly incorporated into the model to reduce uncertainty in the tissue residue predictions. It also allows simulations of the effect of altered organ function (e.g., due to disease states or other physiological variables) on tissue drug residues and WDIs. Population variability can also be incorporated into the model as was done in our study, which makes such population PBPK modeling a useful tool for application in veterinary medicine and food safety assessment.

One of the important features of a PBPK model is that the model is based on mechanistic information of drug action. For the liberation of procaine penicillin G, the rate-limiting step is the hydrolysis of penicillin from the procaine moiety. In current PBPK model,

a two-compartment dissolution model was applied to simulate the dissolution-controlled depot of procaine penicillin G (Bari, 2010). Both the empirical two-compartment model (Leavens et al., 2012) and the mechanistic two-compartment model (Lin et al., 2015) can well simulate the dissolution process of procaine penicillin G. The mechanistic two-compartment model was incorporated into the current PBPK model, as the most realistic approach. The previous PBPK model (Tsuiji et al., 1983) for penicillin G in rats did not consider the dissolution process of penicillin G. Our current model with the liberation process for clinically used formulations of penicillin G can better predict the concentrations of tissue residues.

From the pharmacokinetic data and model simulation results, the concentrations of penicillin G in kidney tissues in swine are higher than all other edible tissues. This may be because penicillin G is eliminated mainly through the urinary pathway (Barza and Weinstein, 1976; Papich and Riviere, 2009). On the contrary, in cattle the highest concentrations of tissue residues were found in liver. In other studies, cattle livers were also identified to hold the highest residue concentrations of penicillin G (Adesokan et al., 2013; Musser et al., 2001). The reason for this species difference is not known.

From the sensitivity analysis results, the uncertainties of many

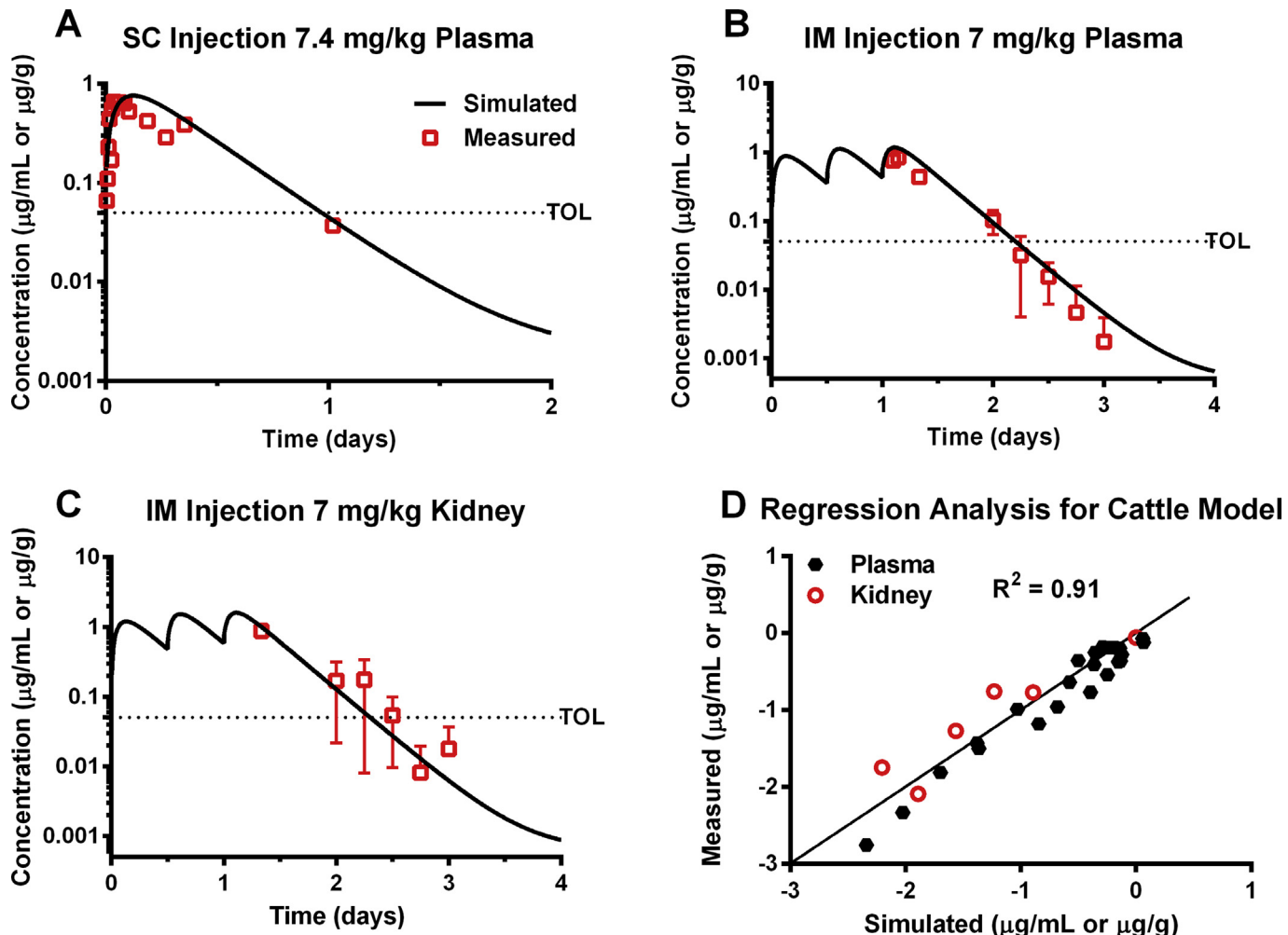


Fig. 5. Evaluation and regression analysis of the cattle model. Comparison of model predictions (solid line) and observed data (red squares) for penicillin G concentrations in the plasma and kidney of cattle exposed to procaine penicillin G via SC single dose (7.4 mg/kg, A), IM repeated 3 doses (7 mg/kg, B, C) is shown. The pharmacokinetic data of panel A and panels B and C are from the studies of Trolldenier et al. (1986) and Chiesa et al. (2006), respectively. Tolerance (TOL) of penicillin G (0.05 µg/g) is shown on three of the panels using dotted line. Panel D represents the result of a regression analysis between log-transformed values of model-simulated and measured penicillin G concentrations for cattle model. R^2 value and the regression line are shown in the panel. (For interpretation of the references to colour in this figure legend, the reader is referred to the web version of this article.)

parameters have influences on the predictions of penicillin concentrations. The variations of physiological parameters have less impact on model simulation results. The partition coefficients of muscle, liver and kidney were highly influential on the prediction of the tissue concentrations. The kidney and muscle partition coefficients in swine and cattle were comparable (kidney: within two fold difference; muscle: within five fold difference) to the experimental values from previous PBPK model in rats (Tsuiji et al., 1983). The partition coefficient for liver of swine was comparable to the value in rats (within three fold difference). The hepatic metabolic rate and urine clearance rate also have impacts on the model predictions. The urinary clearance rates of swine and cattle are comparable (within 2-fold difference) with the reported clearance rates in sheep (0.55 L/h/kg) and horses (0.51 L/h/kg) (Firth et al., 1990; Oukessou et al., 1990; USP, 2007). The hepatic metabolic rate in swine is comparable with reported value in rats (around five-fold difference) (Tsuiji et al., 1979). However, the liver partition coefficient and hepatic metabolic rate in cattle were different from the values in either swine or rats (more than 10-time difference). The reasons for the species-dependent partition coefficients and hepatic metabolism rates are unknown, but it may be due to species differences in tissue composition, metabolism, elimination, and

protein binding of penicillin G (Keen, 1965).

The Monte Carlo sampling technique was applied for the population analysis in this PBPK model. Previous population analysis in PBPK models for veterinary medicines (Buur et al., 2006; Henri et al., 2016; Huang et al., 2015; Yang et al., 2012) was performed only for the sensitive parameters and in acslX, a software program that was discontinued in 2015. For the current model, variations of all physiological and chemical-specific parameters were considered in the Monte Carlo analysis to more accurately simulate the range of tissue residue concentrations in a diverse population. This strategy of population analysis has been applied for PBPK modeling in human drugs and environmental pollutants (Shankaran et al., 2013; Yang et al., 2015b, 2016). Another unique strength of the present Monte Carlo analysis is that the distributions and variabilities of physiological parameters were collected, to the extent possible, directly from or calculated based on original experimental data. The default coefficients of variance were used only for parameters with no experimental data available. There are many published PBPK models using Berkeley Madonna for environmental chemicals, drugs, and nanomaterials, but to the best of our knowledge this is the first PBPK model using Berkeley Madonna to do Monte Carlo analysis. The present Monte Carlo analysis, considering variances of

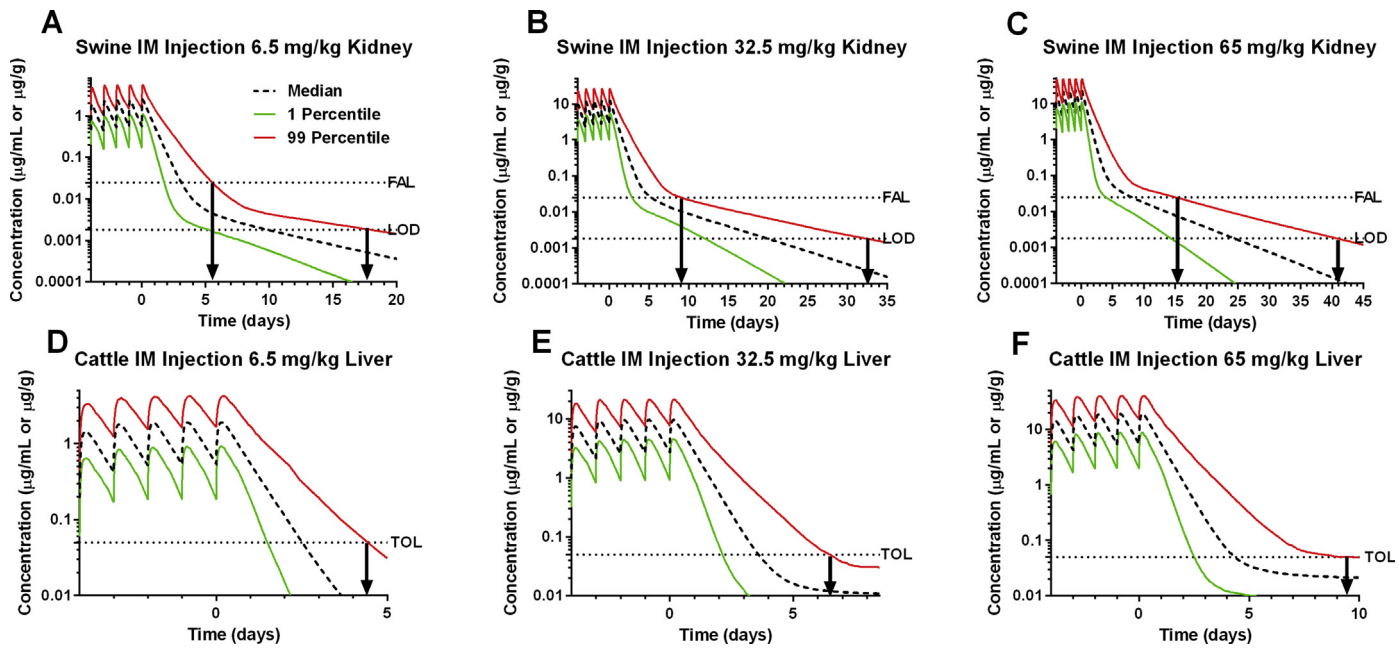


Fig. 6. Monte Carlo simulation for penicillin G concentrations in swine and cattle. Label dose (6.5 mg/kg) and commonly used extralabel dose (5 × label dose, 32.5 mg/kg; 10 × label dose, 65 mg/kg) with 5 repeated doses via IM injection were simulated as the therapeutic scenarios for both swine and cattle. Each of the simulations was run for 1000 iterations. The median, 1th and 99th percentiles of simulated results were plotted without confidence intervals. Results of Monte Carlo analysis in kidney for swine are shown in upper panels (6.5 mg/kg, A; 32.5 mg/kg, B; 65 mg/kg, C). Monte Carlo simulation results for cattle in liver are shown in lower panels (6.5 mg/kg, D; 32.5 mg/kg, E; 65 mg/kg, F). Limit of detection (LOD) and FSIS action limit (FAL) are shown on each of the upper three panels using dotted lines. LOD for the kidney in swine is 1.8 ng/g, and FSIS action limit for penicillin G in swine is 25 ng/g. Tolerance (TOL) of penicillin G (0.05 $\mu\text{g/g}$) is shown on lower panels using dotted line. (For interpretation of the references to colour in this figure legend, the reader is referred to the web version of this article.)

all parameters, may help make the simulations more realistic for the population of livestock treated with drug.

Current population PBPK model can be extrapolated to simulate the extralabel use scenarios of penicillin G. As the frequently used extralabel doses are much higher than label dose of penicillin G to assure continued antimicrobial efficacy against today's less susceptible pathogens, the labeled withdrawal period may not well prevent residue violations. For the label dose, the WDIs for both swine and cattle from Monte Carlo analysis based on tolerance or FSIS action limit were the same or very close (e.g., predicted 5 days vs. label withdrawal period 4 days in cattle) to FDA label withdrawal periods. For extralabel doses, the WDIs in cattle predicted by the current model (7 days for 5 × label dose and 10 days for 10 × label dose) are comparable to the results from the previously published popPK model (7 days for 5 × extralabel dose) (Li et al., 2014). As zero tolerance limits were established for edible tissues in swine, the LOD was used to determine the WDIs. For the label and extralabel use of penicillin G in swine, the WDIs predicted from population PBPK model based on LOD are much longer than the label withdrawal period. With the improvement of analytical chemistry techniques, the LOD of penicillin G in recent studies was lower than previous studies decades ago. The predict WDIs of extralabel doses from the current model are more protective to avoid violative tissue residues of penicillin G in swine and cattle. Estimation of the pharmacokinetic features of drugs near the terminal phase is important for reducing violations of drug residues in edible tissues, as well as for food-producing animals destined to export to more countries with stringent residue criteria.

The current PBPK model was established based on available pharmacokinetic data of procaine penicillin G in market-age swine and adult cattle via IM and SC injections. Limited datasets in piglets and calves were also included in our simulations (Table 1). Our model seems to simulate the kinetics of procaine penicillin G well

in both young and adult animals. However, additional data, especially data in young animals, once available, may be incorporated into this model to help improve the population predictions and to determine the age-dependent pharmacokinetics of procaine penicillin G in swine and cattle. Some of the methods, such as sensitivity and population analysis, can also be optimized to facilitate the establishment of more robust population PBPK models. The local sensitivity analysis is easy and rapid to perform for the large number of parameters involved in PBPK models. The assumptions behind using this method is that the interactions between parameters are negligible, which generally is not true (McNally et al., 2011). The global sensitivity analysis can be applied for the PBPK model to avoid the weakness of the current analysis. Similarly, the Monte Carlo analysis used also did not consider the correlation or covariance between parameters. The application of more advanced Bayesian method via Markov chain Monte Carlo (MCMC) simulations can help avoid this problem (Krauss et al., 2013). The global sensitivity analysis and MCMC simulation will be adapted in our future studies.

In summary, the present PBPK model of penicillin G adequately simulates observed concentrations of penicillin G residues in edible tissues of swine and cattle following IM and SC administrations. The application of the population PBPK model via Monte Carlo simulations to estimate the WDIs for extralabel use of penicillin G demonstrates the possibility to use PBPK modeling to provide more protective WDIs. This PBPK model provides a foundation for application of Berkeley Madonna to establish population PBPK models for other veterinary drugs to predict tissue residues and extended WDIs after extralabel uses.

Conflict of interest statement

The authors declare no conflict of interest.

Acknowledgements

This work was supported by the United States Department of Agriculture National Institute of Food and Agriculture for the Food Animal Residue Avoidance Databank (FARAD) Program (USDA-NIFA-EXCA-005457) and The Kansas Bioscience Authority funds to the Institute of Computational Comparative Medicine (ICCM) at Kansas State University. We would like to acknowledge Dr. Mathias Devreese, Dr. Pritam Sidhu, Dr. Dongping Zeng, and Shiqiang Jin in the Institute of Computational Comparative Medicine at Kansas State University for helpful discussions.

Appendix A. Supplementary data

Supplementary data related to this article can be found at <http://dx.doi.org/10.1016/j.fct.2017.06.023>.

Transparency document

Transparency document related to this article can be found online at <http://dx.doi.org/10.1016/j.fct.2017.06.023>.

References

- Adesokan, H.K., Agada, C.A., Adetunji, V.O., Akanbi, I.M., 2013. Oxytetracycline and penicillin-G residues in cattle slaughtered in south-western Nigeria: implications for livestock disease management and public health. *J. S Afr. Vet. Assoc.* 84, E1–E5.
- Andersen, M.E., 2003. Toxicokinetic modeling and its applications in chemical risk assessment. *Toxicol. Lett.* 138, 9–27.
- Apley, M., Coetzee, H., Gehring, R., Karriker, L., 2009. Pharmacokinetics and tissue residues of procaine penicillin G in sows after administration of 33,000 IU/kg intramuscularly and by needle-free injection in the hip. *Natl. Pork Board Res. Rep. NPB* 07–234.
- Armstrong, R.B., Delp, M.D., Goljan, E.F., Laughlin, M.H., 1987. Distribution of blood flow in muscles of miniature swine during exercise. *J. Appl. Physiol.* 62, 1285–1298.
- Bari, H., 2010. A prolonged release parenteral drug delivery system—an overview. *Int. J. Pharm. Sci. Rev. Res.* 3, 1–11.
- Barza, M., Weinstein, L., 1976. Pharmacokinetics of the penicillins in man. *Clin. Pharmacokinet.* 1, 297–308.
- Bateman, K.G., Martin, S.W., Shewen, P.E., Menzies, P.I., 1990. An evaluation of antimicrobial therapy for undifferentiated bovine respiratory disease. *Can. Vet. J.* 31, 689–696.
- Baynes, R., Riviere, J.E., 2014. Importance of veterinary drug residues. In: Baynes, R., Riviere, J.E. (Eds.), *Strategies for Reducing Drug and Chemical Residues in Food Animals: International Approaches to Residue Avoidance, Management, and Testing*. Wiley, New York, USA, pp. 1–8.
- Baynes, R.E., Dedonder, K., Kissell, L., Mzyk, D., Marmulak, T., Smith, G., Tell, L., Gehring, R., Davis, J., Riviere, J.E., 2016. Health concerns and management of select veterinary drug residues. *Food Chem. Toxicol.* 88, 112–122.
- Brocklebank, J.R., Namdar, R., Law, F.C., 1997. An oxytetracycline residue depletion study to assess the physiologically based pharmacokinetic (PBPK) model in farmed Atlantic salmon. *Can. Vet. J.* 38, 645–646.
- Brynes, S.D., 2005. Demystifying 21 CFR Part 556—tolerances for residues of new animal drugs in food. *Regul. Toxicol. Pharmacol.* 42, 324–327.
- Buur, J., Baynes, R., Smith, G., Riviere, J., 2006. Use of probabilistic modeling within a physiologically based pharmacokinetic model to predict sulfamethazine residue withdrawal times in edible tissues in swine. *Antimicrob. Agents Chemother.* 50, 2344–2351.
- Buur, J.L., Baynes, R.E., Craigmill, A.L., Riviere, J.E., 2005. Development of a physiologic-based pharmacokinetic model for estimating sulfamethazine concentrations in swine and application to prediction of violative residues in edible tissues. *Am. J. Vet. Res.* 66, 1686–1693.
- Buur, J.L., Baynes, R.E., Riviere, J.E., 2008. Estimating meat withdrawal times in pigs exposed to melamine contaminated feed using a physiologically based pharmacokinetic model. *Regul. Toxicol. Pharmacol.* 51, 324–331.
- Buur, J.L., Baynes, R.E., Smith, G.W., Riviere, J.E., 2009. A physiologically based pharmacokinetic model linking plasma protein binding interactions with drug disposition. *Res. Vet. Sci.* 86, 293–301.
- Cao, Y., Jusko, W.J., 2012. Applications of minimal physiologically-based pharmacokinetic models. *J. Pharmacokin. Pharmacodyn.* 39, 711–723.
- Chiesa, O.A., Von Bredow, J., Smith, M., Heller, D., Condon, R., Thomas, M.H., 2006. Bovine kidney tissue/biological fluid correlation for penicillin. *J. Vet. Pharmacol. Ther.* 29, 299–306.
- Clewell 3rd, H.J., Gentry, P.R., Covington, T.R., Gearhart, J.M., 2000. Development of a physiologically based pharmacokinetic model of trichloroethylene and its metabolites for use in risk assessment. *Environ. Health Perspect.* 108 (Suppl. 2), 283–305.
- Clewell, R.A., Clewell III, H.J., 2008. Development and specification of physiologically based pharmacokinetic models for use in risk assessment. *Regul. Toxicol. Pharmacol.* 50, 129–143.
- Cole, M., Kenig, M.D., Hewitt, V.A., 1973. Metabolism of penicillins to penicilloic acids and 6-aminopenicillanic acid in man and its significance in assessing penicillin absorption. *Antimicrob. Agents Chemother.* 3, 463–468.
- Cortright, K.A., Wetzlitz, S.E., Craigmill, A.L., 2009. A PBPK model for midazolam in four avian species. *J. Vet. Pharmacol. Ther.* 32, 552–565.
- Covington, T.R., Robinan Gentry, P., Van Landingham, C.B., Andersen, M.E., Kester, J.E., Clewell, H.J., 2007. The use of Markov chain Monte Carlo uncertainty analysis to support a Public Health Goal for perchloroethylene. *Regul. Toxicol. Pharmacol.* 47, 1–18.
- Craigmill, A.L., 2003. A physiologically based pharmacokinetic model for oxytetracycline residues in sheep. *J. Vet. Pharmacol.* 26, 55–63.
- Craigmill, A.L., Riviere, J.E., Webb, A.I., 2006. Tabulation of FARAD Comparative and Veterinary Pharmacokinetic Data. Blackwell Pub., Ames, USA, pp. 1–1935.
- Dayan, A.D., 1993. Allergy to antimicrobial residues in food: assessment of the risk to man. *Vet. Microbiol.* 35, 213–226.
- Doornenbal, H., Tong, A.K., Sather, A.P., 1986. Relationships among serum characteristics and performance and carcass traits in growing pigs. *J. Anim. Sci.* 62, 1675–1681.
- Doyle, J.T., Patterson, J.L., Warren, J.V., Detweiler, D.K., 1960. Observations on the circulation of domestic cattle. *Circ. Res.* 8, 4–15.
- DrugBank, 2016. Benzylpenicillin. Updated on December 08, 2016 ed. <https://www.drugbank.ca/drugs/DB01053>.
- FDA, 2013a. Guidance for Industry #209, the Judicious Use of Medically Important Antimicrobial Drugs in Food-producing Animals. <https://www.fda.gov/downloads/AnimalVeterinary/GuidanceComplianceEnforcement/GuidanceforIndustry/UCM216936.pdf>.
- FDA, 2013b. Penicillin G Procaine Implantation and Injectable Dosage Forms. Code of Federal Regulations. 21 CFR 522.1696. <https://www.gpo.gov/fdsys/pkg/CFR-2013-title21-vol6/pdf/CFR-2013-title21-vol6-chapI-subchapE.pdf>.
- FDA, 2015. Guidance for Industry# 213, New Animal Drugs and New Animal Drug Combination Products Administered in or on Medicated Feed or Drinking Water of Food-producing Animals: Recommendations for Drug Sponsors for Voluntarily Aligning Product Use Conditions with GFI# 209. <https://www.fda.gov/downloads/AnimalVeterinary/GuidanceComplianceEnforcement/GuidanceforIndustry/UCM299624.pdf>.
- FDA, 2016a. FDA Reminds Retail Establishments of Upcoming Changes to the Use of Antibiotics in Food Animals. <http://www.fda.gov/AnimalVeterinary/NewsEvents/CVMUpdates/ucm507355.htm>.
- FDA, 2016b. Guidance for Industry #3, General Principles for Evaluating the Human Food Safety of New Animal Drugs Used in Food-producing Animals. <https://www.fda.gov/downloads/AnimalVeterinary/GuidanceComplianceEnforcement/GuidanceforIndustry/UCM052180.pdf>.
- FDA, 2017. Code of Federal Regulations 21, CFR Parts 530.3. <https://www.accessdata.fda.gov/scripts/cdrh/cfdocs/cfr/CFRSearch.cfm?fr=530.3>.
- Firth, E., Nouws, J., Klein, W., Driessens, F., 1990. The effect of phenylbutazone on the plasma disposition of penicillin G in the horse. *J. Vet. Pharmacol. Ther.* 13, 179–185.
- Fisher, J.W., 2000. Physiologically based pharmacokinetic models for trichloroethylene and its oxidative metabolites. *Environ. Health Perspect.* 108, 265–273.
- FSIS, 2013. Screening and Confirmation of Animal Drug Residues by UHPLC-MS-MS. <https://www.fsis.usda.gov/wps/wcm/connect/b9d45c8b-74d4-4e99-8eda-5453812eb237/CLG-MRM1.pdf?MOD=AJPERES>.
- Gelman, A., Bois, F., Jiang, J., 1996. Physiological pharmacokinetic analysis using population modeling and informative prior distributions. *J. Am. Stat. Assoc.* 91, 1400–1412.
- Gomes, E.R., Demoly, P., 2005. Epidemiology of hypersensitivity drug reactions. *Curr. Opin. Allergy Clin. Immunol.* 5, 309–316.
- Gujer, W., 2008a. Measurement and Measurement Uncertainty, Systems Analysis for Water Technology. Springer Berlin Heidelberg, Berlin, Heidelberg, pp. 237–255.
- Gujer, W., 2008b. Parameter Identification, Sensitivity and Error Propagation, Systems Analysis for Water Technology. Springer Berlin Heidelberg, Berlin, Heidelberg, pp. 257–313.
- Hannon, J.P., Bossone, C., Wade, C., 1990. Normal physiological values for conscious pigs used in biomedical research. *Lab. Anim. Sci.* 40, 293–298.
- Henri, J., Carrez, R., Méda, B., Laurentie, M., Sanders, P., 2016. A physiologically based pharmacokinetic model for chickens exposed to feed supplemented with monensin during their lifetime. *J. Vet. Pharmacol. Ther.* <http://onlinelibrary.wiley.com/doi/10.1111/jvp.12370/abstract> [Epub ahead of print].
- Huang, L., Lin, Z., Zhou, X., Zhu, M., Gehring, R., Riviere, J.E., Yuan, Z., 2015. Estimation of residue depletion of cyadox and its marker residue in edible tissues of pigs using physiologically based pharmacokinetic modelling. *Food Addit. Contam. Part A Chem. Anal. Control Expo. Risk Assess.* 32, 2002–2017.
- Keen, P.M., 1965. The binding of three penicillins in the plasma of several mammalian species as studied by ultrafiltration at body temperature. *Br. J. Pharmacol. Chemother.* 25, 507–514.
- Kerr, R.A., Bartol, T.M., Kaminsky, B., Dittrich, M., Chang, J.-C.J., Baden, S.B., Sejnowski, T.J., Stiles, J.R., 2008. Fast Monte Carlo simulation methods for biological reaction-diffusion systems in solution and on surfaces SIAM. *J. Sci. Comput.* 30, 3126–3126.

- Komatsu, T., Inomata, T., Watanabe, I., Kobayashi, M., Kokubun, H., Ako, J., Atsuda, K., 2016. Population pharmacokinetic analysis and dosing regimen optimization of penicillin G in patients with infective endocarditis. *J. Pharm. Health Care Sci.* 2, 9.
- Korsrud, G.O., Boison, J.O., Papich, M.G., Yates, W.D., MacNeil, J.D., Janzen, E.D., Cohen, R.D., Landry, D.A., Lambert, G., Yong, M.S., et al., 1993. Depletion of intramuscularly and subcutaneously injected procaine penicillin G from tissues and plasma of yearling beef steers. *Can. J. Vet. Res.* 57, 223–230.
- Korsrud, G.O., Papich, M.G., Fesser, A.C.E., Salisbury, C.D.C., MacNeil, J.D., 1996. Residue depletion in tissues and fluids from swine fed sulfamethazine, chlorotetracycline and penicillin G in combination. *Food Addit. Contam.* 13, 287–292.
- Korsrud, G.O., Salisbury, C.D., Rhodes, C.S., Papich, M.G., Yates, W.D., Bulmer, W.S., MacNeil, J.D., Landry, D.A., Lambert, G., Yong, M.S., Ritters, L., 1998. Depletion of penicillin G residues in tissues, plasma and injection sites of market pigs injected intramuscularly with procaine penicillin G. *Food Addit. Contam.* 15, 421–426.
- Krause, A., Lowe, P.J., 2014. Visualization and communication of pharmacometric models with berkeley madonna. *CPT Pharmacometrics Syst. Pharmacol.* 3, e116.
- Krauss, M., Burghaus, R., Lippert, J., Niemi, M., Neuvonen, P., Schuppert, A., Willmann, S., Kuepfer, L., Görlitz, L., 2013. Using Bayesian-PBPK modeling for assessment of inter-individual variability and subgroup stratification. *Silico Pharmacol* 1, 6.
- Krishnan, K., Crouse, L.C., Bazar, M.A., Major, M.A., Reddy, G., 2009. Physiologically based pharmacokinetic modeling of cyclotrimethylenetrinitramine in male rats. *J. Appl. Toxicol.* 29, 629–637.
- Kukanich, B., Gehring, R., Webb, A.I., Craigmill, A.L., Riviere, J.E., 2005. Effect of formulation and route of administration on tissue residues and withdrawal times. *J. Am. Vet. Med. Assoc.* 227, 1574–1577.
- Leavens, T.L., Tell, L.A., Clothier, K.A., Griffith, R.W., Baynes, R.E., Riviere, J.E., 2012. Development of a physiologically based pharmacokinetic model to predict tulathromycin distribution in goats. *J. Vet. Pharmacol. Ther.* 35, 121–131.
- Leavens, T.L., Tell, L.A., Kissell, L.W., Smith, G.W., Smith, D.J., Wagner, S.A., Shelver, W.L., Wu, H., Baynes, R.E., Riviere, J.E., 2014. Development of a physiologically based pharmacokinetic model for flunixin in cattle (*Bos taurus*). *Food Addit. Contam. Part A Chem. Anal. Control Expo. Risk Assess.* 31, 1506–1521.
- Lescoat, P., Sauvant, D., Danfaer, A., 1996. Quantitative aspects of blood and amino acid flows in cattle. *Reprod. Nutr. Dev.* 36, 137–174.
- Li, M., Gehring, R., Lin, Z., Riviere, J., 2015. A framework for meta-analysis of veterinary drug pharmacokinetic data using mixed effect modeling. *J. Pharm. Sci.* 104, 1230–1239.
- Li, M., Gehring, R., Tell, L., Baynes, R., Huang, Q., Riviere, J.E., 2014. Interspecies mixed-effect pharmacokinetic modeling of penicillin G in cattle and swine. *Antimicrob. Agents Chemother.* 58, 4495–4503.
- Lin, Z., Fisher, J.W., Ross, M.K., Filipov, N.M., 2011. A physiologically based pharmacokinetic model for atrazine and its main metabolites in the adult male C57BL/6 mouse. *Toxicol. Appl. Pharmacol.* 251, 16–31.
- Lin, Z., Fisher, J.W., Wang, R., Ross, M.K., Filipov, N.M., 2013. Estimation of placental and lactational transfer and tissue distribution of atrazine and its main metabolites in rodent dams, fetuses, and neonates with physiologically based pharmacokinetic modeling. *Toxicol. Appl. Pharmacol.* 273, 140–158.
- Lin, Z., Gehring, R., Mochel, J.P., Lave, T., Riviere, J.E., 2016a. Mathematical modeling and simulation in animal health - Part II: principles, methods, applications, and value of physiologically based pharmacokinetic modeling in veterinary medicine and food safety assessment. *J. Vet. Pharmacol. Ther.* 39, 421–438.
- Lin, Z., Jaber-Douraki, M., He, C., Jin, S., Yang, R.S., Fisher, J.W., Riviere, J.E., 2017. Performance assessment and translation of physiologically based pharmacokinetic models from acslX to berkeley madonna, MATLAB(R), and R language: oxytetracycline and gold nanoparticles as case examples. *Toxicol. Sci.* <https://doi.org/10.1093/toxsci/kfx070> [Epub ahead of print].
- Lin, Z., Li, M., Gehring, R., Riviere, J.E., 2015. Development and application of a multiroute physiologically based pharmacokinetic model for oxytetracycline in dogs and humans. *J. Pharm. Sci.* 104, 233–243.
- Lin, Z., Vahl, C.I., Riviere, J.E., 2016b. Human food safety implications of variation in food animal drug metabolism. *Sci. Rep.* 6, 27907.
- Lundeen, G., Manohar, M., Parks, C., 1983. Systemic distribution of blood flow in swine while awake and during 1.0 and 1.5 MAC isoflurane anesthesia with or without 50% nitrous oxide. *Anesth. Analg.* 62, 499–512.
- Lupton, S.J., Shelver, W.L., Newman, D.J., Larsen, S., Smith, D.J., 2014. Depletion of penicillin G residues in heavy sows after intramuscular injection. Part I: tissue residue depletion. *J. Agric. Food Chem.* 62, 7577–7585.
- Macey, R., Oster, G., Zahnley, T., 2009. Berkeley Madonna User's Guide Version 8.0.2. University of California, Berkeley, CA, pp. 1–70.
- Martin-Jimenez, T., Riviere, J.E., 1998. Population pharmacokinetics in veterinary medicine: potential use for therapeutic drug monitoring and prediction of tissue residues. *J. Vet. Pharmacol. Ther.* 21, 167–189.
- McNally, K., Cotton, R., Loizou, G.D., 2011. A workflow for global sensitivity analysis of PBPK models. *Front. Pharmacol.* 2, 31.
- Mirfazaelian, A., Kim, K.-B., Anand, S.S., Kim, H.J., Tornero-Velez, R., Bruckner, J.V., Fisher, J.W., 2006. Development of a physiologically based pharmacokinetic model for deltamethrin in the adult male sprague-dawley rat. *Toxicol. Sci.* 93, 432–442.
- Mirzaei, H.R., Pitchford, W.S., Verbyla, A.P., 2011. Modeling of crossbred cattle growth, comparison between cubic and piecewise random regression models. *Genet. Mol. Res.* 10, 2230–2244.
- Musser, J.M., Anderson, K.L., Boison, J.O., 2001. Tissue disposition and depletion of penicillin G after oral administration with milk in unweaned dairy calves. *J. Am. Vet. Med. Assoc.* 219, 346–350.
- Nestorov, I.A., Aarons, L.J., Arundel, P.A., Rowland, M., 1998. Lumping of whole-body physiologically based pharmacokinetic models. *J. Pharmacokinet. Biopharm.* 26, 21–46.
- Oukessou, M., Hossaini, J., Zine-Filali, R., Toutain, P.L., 1990. Comparative benzylpenicillin pharmacokinetics in the dromedary *Camelus dromedarius* and in sheep. *J. Vet. Pharmacol. Ther.* 13, 298–303.
- Papich, M.G., Korsrud, G.O., Boison, J.O., Yates, W.D., MacNeil, J.D., Janzen, E.D., Cohen, R.D., Landry, D.A., 1993. A study of the disposition of procaine penicillin G in feedlot steers following intramuscular and subcutaneous injection. *J. Vet. Pharmacol. Ther.* 16, 317–327.
- Papich, M.G., Riviere, J.E., 2009. Lactam antibiotics: PENICILLINS, cephalosporins, and related drugs. In: Riviere, J.E., Papich, M.G. (Eds.), *Veterinary Pharmacology and Therapeutics*, ninth ed. Wiley, Ames, USA, pp. 866–888.
- Payne, M.A., Craigmill, A., Riviere, J.E., Webb, A.I., 2006. Extralabel use of penicillin in food animals. *J. Am. Vet. Med. Assoc.* 229, 1401–1403.
- Phuc, B.H.N., Hieu, L.T., 1993. A molasses in diets for growing pigs. *Livest. Res. Rural Dev.* 5, 11–15.
- Poet, T.S., Schlosser, P.M., Rodriguez, C.E., Parod, R.J., Rodwell, D.E., Kirman, C.R., 2016. Using physiologically based pharmacokinetic modeling and benchmark dose methods to derive an occupational exposure limit for N-methylpyrrolidone. *Regul. Toxicol. Pharmacol.* 76, 102–112.
- Portis, E., Lindeman, C., Johansen, L., Stoltman, G., 2012. A ten-year (2000–2009) study of antimicrobial susceptibility of bacteria that cause bovine respiratory disease complex—mannheimia haemolytica, pasteurella multocida, and *histophilus somni*—in the United States and Canada. *J. Vet. Diagn. Invest.* 24, 932–944.
- Raison-Peyron, N., Messaad, D., Bousquet, J., Demoly, P., 2001. Anaphylaxis to beef in penicillin-allergic patient. *Allergy* 56, 796–797.
- Ranheim, B., Ween, H., Egeli, A.K., Hormazabal, V., Yndestad, M., Soli, N.E., 2002. Benzathine penicillin G and procaine penicillin G in piglets: comparison of intramuscular and subcutaneous injection. *Vet. Res. Commun.* 26, 459–465.
- Riviere, J.E., Craigmill, A.L., Sundlof, S.F., 1986. Food animal residue avoidance Databank (FARAD): an automated pharmacologic Databank for drug and chemical residue avoidance. *J. Food Prot.* 49, 826–830.
- Riviere, J.E., Tell, L.A., Baynes, R.E., Vickroy, T.W., Gehring, R., 2017. Guide to FARAD resources: historical and future perspectives. *J. Am. Vet. Med. Assoc.* 250, 1131–1139.
- Shankaran, H., Adeshina, F., Teeguarden, J.G., 2013. Physiologically-based pharmacokinetic model for fentanyl in support of the development of provisional advisory levels. *Toxicol. Appl. Pharmacol.* 273, 464–476.
- Shi, Z., Chapes, S.K., Ben-Arieh, D., Wu, C.-H., 2016. An agent-based model of a hepatic inflammatory response to *Salmonella*: a computational study under a large set of experimental data. *PLoS One* 11, e0161131.
- Sterner, T.R., Ruark, C.D., Covington, T.R., Yu, K.O., Gearhart, J.M., 2013. A physiologically based pharmacokinetic model for the oxime TMB-4: simulation of rodent and human data. *Arch. Toxicol.* 87, 661–680.
- Swett WW, M.F., Graves, R.R., Matthews, C.A., 1933. Variations Recorded in the Study of the Conformation and Anatomy of 318 Dairy Cows Having Records of Production. Memo. Pub. BDIM—589. Bureau of Dairy Industry, Division of Dairy Cattle and Cattle Breeding, Feeding, and Management, Washington (DC): United States.
- Tan, Y.M., Liao, K.H., Conolly, R.B., Blount, B.C., Mason, A.M., Clewell, H.J., 2006. Use of a physiologically based pharmacokinetic model to identify exposures consistent with human biomonitoring data for chloroform. *J. Toxicol. Environ. Health Part A* 69, 1727–1756.
- Tranquilli, W.J., Parks, C.M., Thurmon, J.C., Benson, G.J., Koritz, G.D., Manohar, M., Theodorakis, M.C., 1982. Organ blood flow and distribution of cardiac output in nonanesthetized swine. *Am. J. Vet. Res.* 43, 895–897.
- Trolldenier, H., Ratzinger, S., Bache, K., Amm, H., Dubrow, R., 1986. Blood levels, pharmacokinetics and residualization of benzylpenicillin Ursopen 100000 in calves following subcutaneous injection. *Monatsh. Veterinärmed.* 41, 435–411.
- Tsuji, A., Miyamoto, E., Terasaki, T., Yamana, T., 1979. Physiological pharmacokinetics of Mactam antibiotics: penicillin V distribution and elimination after intravenous administration in rats. *J. Pharm. Pharmacol.* 31, 116–119.
- Tsuji, A., Yoshikawa, T., Nishide, K., Minami, H., Kimura, M., Nakashima, E., Terasaki, T., Miyamoto, E., Nightingale, C.H., Yamana, T., 1983. Physiologically based pharmacokinetic model for β-lactam antibiotics I: tissue distribution and elimination rates. *J. Pharm. Sci.* 72, 1239–1252.
- Uboh, C.E., Soma, L.R., Luo, Y., McNamara, E., Fennell, M.A., May, L., Teleis, D.C., Rudy, J.A., Watson, A.O., 2000. Pharmacokinetics of penicillin G procaine versus penicillin G potassium and procaine hydrochloride in horses. *Am. J. Vet. Res.* 61, 811–815.
- Upton, R.N., 2008. Organ weights and blood flows of sheep and pig for physiological pharmacokinetic modelling. *J. Pharmacol. Toxicol. Methods* 58, 198–205.
- USDA, 2015. U.S. National Residue Program: 2014 Residue Sample Results. <http://www.fsis.usda.gov/wps/wcm/connect/2428086b-f8ec-46ed-8531-a45d10bfef6/2014-Res-Book.pdf?MOD=AJPERES>.
- USP, 2007. PENICILLIN G (Veterinary—systemic) Veterinary Antibiotic Monographs. www.aacpt.org/resource/resmgr/imported/penicillinG.pdf.
- Vogel, G., Nicolet, J., Martig, J., Tschudi, P., Meylan, M., 2001. Pneumonia in calves: characterization of the bacterial spectrum and the resistance patterns to antimicrobial drugs. *Schweiz. Arch. Tierheilkd* 143, 341–350.
- WHO, 2010. Characterization and Application of Physiologically Based

- Pharmacokinetic Models in Risk Assessment. World Health Organization, International Programme on Chemical Safety, Geneva, Switzerland, pp. 1–91. http://www.who.int/ipcs/methods/harmonization/areas/pbpk_models.pdf.
- Wishart, D.S., Knox, C., Guo, A.C., Shrivastava, S., Hassanali, M., Stothard, P., Chang, Z., Woolsey, J., 2006. DrugBank: a comprehensive resource for in silico drug discovery and exploration. *Nucleic Acids Res.* 34, D668–D672.
- Yang, B., Huang, L.L., Fang, K., Wang, Y.L., Peng, D.P., Liu, Z.L., Yuan, Z.H., 2014a. A physiologically based pharmacokinetic model for the prediction of the depletion of methyl-3-quinoxaline-2-carboxylic acid, the marker residue of olaquindox, in the edible tissues of pigs. *J. Vet. Pharmacol. Ther.* 37, 66–82.
- Yang, F., Liu, H.W., Li, M., Ding, H.Z., Huang, X.H., Zeng, Z.L., 2012. Use of a Monte Carlo analysis within a physiologically based pharmacokinetic model to predict doxycycline residue withdrawal time in edible tissues in swine. *Food Addit. Contam. Part A Chem. Anal. Control Expo. Risk Assess.* 29, 73–84.
- Yang, F., Sun, N., Liu, Y.M., Zeng, Z.L., 2015a. Estimating danofloxacin withdrawal time in broiler chickens based on physiologically based pharmacokinetics modeling. *J. Vet. Pharmacol. Ther.* 38, 174–182.
- Yang, F., Sun, N., Sun, Y.X., Shan, Q., Zhao, H.Y., Zeng, D.P., Zeng, Z.L., 2013. A physiologically based pharmacokinetics model for florfenicol in crucian carp and oral-to-intramuscular extrapolation. *J. Vet. Pharmacol. Ther.* 36, 192–200.
- Yang, F., Yang, Y.R., Wang, L., Huang, X.H., Qiao, G., Zeng, Z.L., 2014b. Estimating marbofloxacin withdrawal time in broiler chickens using a population physiologically based pharmacokinetics model. *J. Vet. Pharmacol. Ther.* 37, 579–588.
- Yang, X., Doerge, D.R., Teeguarden, J.G., Fisher, J.W., 2015b. Development of a physiologically based pharmacokinetic model for assessment of human exposure to bisphenol A. *Toxicol. Appl. Pharmacol.* 289, 442–456.
- Yang, X., Duan, J., Fisher, J., 2016. Application of physiologically based absorption modeling to characterize the pharmacokinetic profiles of oral extended release methylphenidate products in adults. *PLoS One* 11, e0164641.
- Yang, X., Zhou, Y.F., Yu, Y., Zhao, D.H., Shi, W., Fang, B.H., Liu, Y.H., 2015c. A physiologically based pharmacokinetic model for quinoxaline-2-carboxylic acid in rats, extrapolation to pigs. *J. Vet. Pharmacol. Ther.* 38, 55–64.
- Yoon, M., Nong, A., Clewell 3rd, H.J., Taylor, M.D., Dorman, D.C., Andersen, M.E., 2009. Evaluating placental transfer and tissue concentrations of manganese in the pregnant rat and fetuses after inhalation exposures with a PBPK model. *Toxicol. Sci.* 112, 44–58.
- Yuan, L.G., Luo, X.Y., Zhu, L.X., Wang, R., Liu, Y.H., 2011. A physiologically based pharmacokinetic model for valnemulin in rats and extrapolation to pigs. *J. Vet. Pharmacol. Ther.* 34, 224–231.
- Zhu, X., Huang, L., Xu, Y., Xie, S., Pan, Y., Chen, D., Liu, Z., Yuan, Z., 2017. Physiologically based pharmacokinetic model for quinocetone in pigs and extrapolation to mequindox. *Food Addit. Contam. Part A Chem. Anal. Control Expo. Risk Assess.* 34, 192–210.